Am J Transl Res 2021;13(5):4376-4388
www.ajtr.org /ISSN:1943-8141/AJTR0116672

Original Article

METTL3 induces bone marrow mesenchymal stem cells osteogenic differentiation and migration through facilitating M1 macrophage differentiation

Hong Lei[3*], Mingyu He[3*], Xiaoqi He[3*], Guanghui Li[3], Yang Wang[2,4], Yuelin Gao[3], Gege Yan[3], Quan Wang[4], Tao Li[3], Guoxin Liu[3], Weijie Du[3,5], Ye Yuan[2,4,5], Lei Yang[1]

[1]Department of Orthopedics, The First Affiliated Hospital of Harbin Medical University, Harbin 150081, China; [2]Department of Pharmacy, The Second Affiliated Hospital of Harbin Medical University, Harbin 150081, China; [3]Department of Pharmacology, College of Pharmacy, Harbin Medical University, Harbin 150081, China; [4]Department of Clinical Pharmacology, College of Pharmacy, Harbin Medical University, Harbin 150081, China; [5]Research Unit of Noninfectious Chronic Diseases in Frigid Zone, Chinese Academy of Medical Sciences, 2019RU070, Harbin 150081, China. [*]Equal contributors.

Received June 20, 2020; Accepted December 11, 2020; Epub May 15, 2021; Published May 30, 2021

Abstract: Despite the crucial role of m^{6}A methyltransferase METTL3 in multiple diseases onset and progression, there are still lacking hard evidence proving that METTL3 could affect macrophage polarization in the stage of bone repair. Here, we aimed to explore the potential involvement of METTL3 in bone repair through modulating macrophage polarization and decipher the underlying cellular/molecular mechanisms. Here we treated RAW 264.7 cells and BM-derived primary macrophages (BMDM) with lipopolysaccharide (LPS) to induce M1 differentiation. METTL3 expression was upregulated in pro-inflammatory macrophages (M1) as compared with macrophages (M0). And overexpression of METTL3 promoted the expression of IL-6 and iNOS secretion by M1 macrophage. In the coculture condition, M1 macrophages with forced expression of METTL3 significantly enhanced migration ability of BMSCs, and also remarkably facilitated osteogenesis ability of BMSCs; the opposite was true when expression of METTL3 was knockdown. In addition, the m^{6}A-RIP microarray suggested that METTL3 silencing significantly reduce the m^{6}A modification of DUSP14, HDAC5 and Nfam1. Furthermore, the findings showed that expression of HADC5 was downregulated in M1 macrophages with METTL3 knockdown, while the DUSP14 expression had slight change and Nfam1 expression was very low. In contrast, METTL3 overexpression promoted HDAC5 expression, indicating that HDAC5 is the critical target gene of METTL3. Under such a theme, we proposed that METTL3 overexpression might be a new approach of replacement therapy for the treatment of bone repair.

Keywords: METTL3, BMSCs, macrophage, osteogenic differentiation, migration

Introduction

Bone fracture healing is a multiply processes including three steps: bone regeneration, porotic stage and remodeling. Bone regeneration begins with the inflammatory reactions of macrophages which interacting with skeletal system via the regulation of bone marrow mesenchymal stem cells (BMSCs) function [1]. Excepting the promotion of inflammatory response occurrence and the local microorganisms removal, accumulating evidence has proved that macrophages make great contributions to bone regeneration due to the mediation of BMSCs osteogenic differentiation and migration ability [2, 3]. Macrophages have at least two subtypes containing classically activated/inflammatory (M1) and alternatively activated regenerative subpopulations (M2), which regulated different cytokines [4, 5]. M1 macrophage exhibits pro-inflammatory functions and secretes inflammatory cytokines such as IL-6, iNOS, TNF-α, IL-1α and IL-1β, while M2 macrophage expresses high anti-inflammatory cytokines including ARG1, IL-10 and so on [6]. Nevertheless, whether the ability to promote bone repair is attributed to M1 or M2 remains a matter of debate. In spite of this, several previ-

ous studies have shown that M1 but not M2 macrophage promotes BMSCs osteogenic differentiation and migration. M1 macrophage involved in bone repair is due to the syntheses of cytokines OSM, TNF-α and IL-6, which have been found to positively affect BMSCs osteogenic differentiation [7-9]. Moreover, there are additional evidence further support that M1 rather than M2 macrophage is more important for the osteogenesis of BMSCs [10, 11].

Methyltransferase-like 3 (METTL3) is the m^6A methyltransferase which binds to METTL14 and wilms tumour 1-associated protein (WTAP) to form a complex catalyzing the m^6A modification, the most abundant epitranscriptomic modification in eukaryotic mRNAs [12]. M^6A modification plays vital role in a variety of human disorders and diseases, such as tumor development, kidney injury, stem cell differentiation and myocardial ischemia [13-16]. Noteworthily, our previous study has shown that silence of METTL3 decreased m^6A methylation levels and inhibited osteogenic differentiation of BMSCs and reduced bone mass [17]. However, the impact of macrophage polarization mediated by m^6A modification on bone regeneration remains incompletely unclear.

Here, we have investigated that M1 macrophage modulated by METTL3 plays a critical role in BMSCs osteogenic differentiation and migration by regulating the expression of its critical target histone deacetylase 5 (HDAC5) through m^6A-based post-transcriptional control.

Methods

Cell culturing and treatment

The mouse macrophage cell line RAW 264.7 was obtained from American Type Culture Collection (ATCC). The RAW 264.7 cell line was cultured in RPMI 1640 medium (Cat#-C22400500BT, GIBCO, Suzhou, China) supplemented with 10% fetal bovine serum (Biological Industries, Israel) and 200U of penicillin/streptomycin (Cat#SV30010, HyClone, California, United States). Macrophage activation was performed using 100 ng/ml lipopolysaccharide (LPS) (Cat. No. L8880, Solarbio). BMSCs from C57BL/6 mice (MUBMX-01001) were purchased from Cyagen (Guangzhou, China) and cultured in BMSC complete medium (MUBMX-90011; Cyagen). For BMDMs, BMSCs were treated with 25 ng/ml M-SCF (Cat#426 ML; R&D Systems, USA) for 7 days, and then incubated with 100 ng/ml LPS for 24 h. All cell lines were maintained in an incubator at 37°C in an atmosphere containing 5% CO_2.

Quantitative real-time polymerase chain reaction (qRT-PCR)

QRT-PCR analysis was performed as described previously. Briefly, total RNA was extracted using TRIzol reagent (Life technologies Corporation) followed the manufacturer's protocol. 500 ng was reverse transcribed to 10 μL cDNA using High Capacity cDNA Reverse Transcription Kit (Cat#00676299; Thermo Fisher Scientific, Waltham, USA). Detection were performed using 7500HT Fast Real-Time PCR System (Applied Biosystems) with SYBR Green PCR master Mix (Cat#31598800; Roche). Gene expression was normalized to endogenous GAPDH mRNA. The primers sequences used as follow: Forward (F)/Reverse (R) primer sequence (5'-3'); IL-6-F: CTGCAAGAGACTTCCATCCAG; IL-6-R: AGTGGTATAGACAGGTCTGTTGG; iNOS-F: CAGCGGAGTGACGGCAAACAT; iNOS-R: GCAAGACCAGAGGCAGCACATC; METTL3-F: CTTTCTACCCCATCTTGAGTG; METTL3-R: CCAACCTTCCGTAGTGATAGTC; Dusp 14-F: CCTTTCCTGCTTTCTTTCTG; Dusp 14-R: GCCCTTGATCTTCCTTAAAC; HDAC5-F: CAAGGCCTTGTGCATGCTGGGCTGG; HDAC5-R: CTGCTCCCGTAGCGCAGGGTCCATG; GAPDH-F: ACTGAGGACCAGGTTGTC; GAPDH-R: TGCTGTAGCCGTATTCATTG.

Western blot

Western blot analysis was performed as described previously. Briefly, washed the cells with PBS, and then lysed on ice for 1 h using RIPA buffer (Beyotime Biotechnology) followed by centrifugation at 13,500 g at 4°C for 15 min. Protein sample (μg) was separated on a polyacrylamide gel, transferred onto a nitrocellulose membrane. The membrane was blocked with 5% fat-free dry milk at room temperature for 1 h. Next, the membrane was incubated with rabbit anti-iNOS antibody (1:500, Cat#ab15323, Abcan), rabbit anti-METTL3 antibody (1:1000, Cat#A8370, ABclonal, Massachusetts, USA) a mouse anti-GAPDH antibody (1:500, Cat#abs830030, Absin) at 4°C for 24 h. All antibodies were diluted in PBS.

Cell transfection

Cells were transfected with siRNA using Lipofectamine RNA iMAX Reagent (MAN0007825, Invitrogen, Carlsbad, California, USA) according to the manufacturer's instructions for 24 h. The sequences of siRNAs used are METTL3: sense 5'-GCUGCACUUCAGACGAAUUTT-3' and antisense 5'-AAUUCGUCUGAAGUGCAGCTT-3'. Using METTL3-carrying plasmid which constructed by Cyagen to elevated the expression of METTL3 in cells. Cells were transfected with 1 μg METTL3 plasmid using X-tremeGENE HP DNA Transfection Reagent (Cat#26540900, Roche, Basel, Switzerland) for 48 h.

BMSC migration analysis

BMSC migration assay was performed with a 24-well transwell chamber (porous polycarbonate membrane with a pore size of 8 μm, Corning Costar). RAW 264.7 cells were cultured in the lower chambers and transfected with siRNA for 24 h and plasmid for 48 h to allow M1 differentiation. BMSCs were seeded in the upper chambers. Co-cultured for 24 h. The membranes were stained with 0.1% crystal violet (Beyotime Biotechnology, China). Six fields were randomly selected and counted using a light microscopy (ECLIPSE TS100, Nikon).

Osteogenic differentiation and Alizarin Red S (ARS) staining

Induced BMSCs into osteoblasts was performed as described previously. Briefly, BMSCs were seeded onto a 6-well plate coated with gelatin (GLT-11301; Cyagen) at a cell density of 2×10^4 cells/cm^2. When the cell confluence reached 60-70%, 2 mL osteogenic differentiation medium (MUBMX-90021; Cyagen) was carefully added to the plate. Differentiation was induced for 7 days, and fresh culture medium was replaced every 3 days. BMSCs were fixed with 4% formaldehyde at RT for 30 min. Cells were washed with PBS three times and then stained with 40 mM Alizarin Red S solution (S0141; Cyagen) for 5 min. Six fields were randomly selected using a light microscopy and calculated using ImageJ software (National Institutes of Health, NIH, USA).

Statistical analysis

Data are expressed as mean ± SEM. Statistical analysis was performed using GraphPad Prism7 software and analyzed with Student's t-test (two-tailed). All experiments were independently repeated at least three times. *P < 0.05; **P < 0.01; ***P < 0.001.

Results

Impact of METTL3 in macrophages polarization

To determine the effects of METTL3 mediated m^{6}A modification in the polarization towards M1 macrophages in bone regeneration, we treated a macrophage cell line RAW 264.7 (M0 macrophage) with lipopolysaccharide (LPS) at 100 ng/μl to induce M1 macrophage (**Figure 1A**). QRT-PCR and western blot results showed the increased expression of M1 macrophage makers iNOS and IL-6, which indicating the M1 differentiation of the RAW 264.7 cells (**Figure 1B**, **1C** and Supplementary Figure 4). We next explored the expression level of METTL3 in M0 and M1 macrophage respectively. Western blot analysis showed that METTL3 protein level was significantly higher in the M1 macrophage compared to M0 macrophage (**Figure 1D** and Supplementary Figure 4). To further investigate the role of METTL3 in macrophage differentiation, we conducted loss-of-function studies in RAW 264.7 cells using METTL3 siRNA. Knockdown efficiency of METTL3 mRNA and protein were detected by qRT-PCR and western blot analysis (**Figure 1E** and Supplementary Figure 4). Consistently, METTL3 silence decreased iNOS and IL-6 mRNA expression level in the presence of LPS, indicating that METTL3 knockdown inhibits the M1 macrophage differentiation (**Figure 1F**).

We then performed gain-of-function studies to confirm whether METTL3 overexpression develop M1 macrophage differentiation. RAW 264.7 cells were transfected with vector and METTL3 plasmid for 24 h and then treated with LPS (100 ng/μl) for 24 h. qRT-PCR and western blot analysis tested the transfection efficiency (**Figure 2A** and Supplementary Figure 4). As expected, forced expression METTL3 promoted the expression of M1 makers iNOS and IL-6 obviously (**Figure 2B**).

Additionally, we also treated bone marrow derived macrophages (BMDM) with LPS (100 ng/μl) to induce M1 macrophage, which were induced from BMSCs in the presence of MSC-F (25 ng/μl) as descripted in **Figure 3A**. M1 mac-

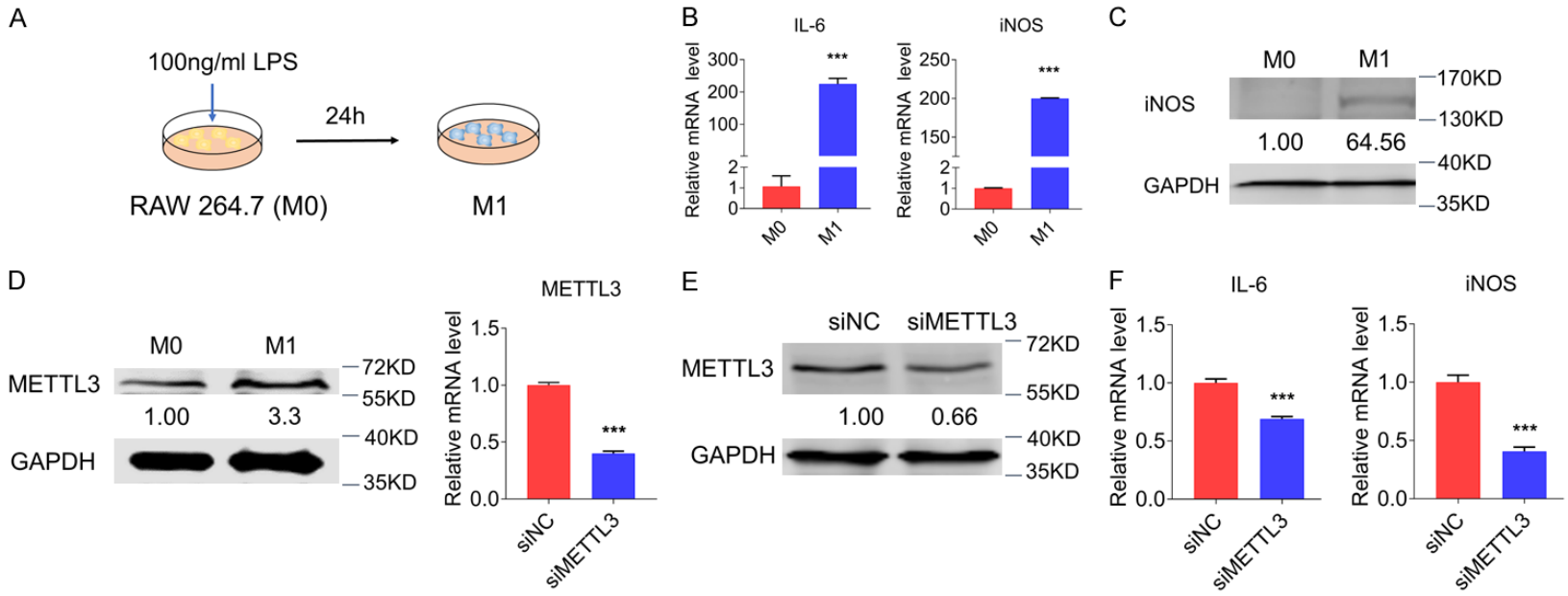

Figure 1. METTL3 play a critical role in M1 macrophage polarization of RAW 264.7 cells. A. The schematic diagram presenting the treatment procedure for M1 macrophage polarization of RAW 264.7 cells. B. qRT-PCR results showing the mRNA expression level of M1 macrophage makers IL-6 and iNOS in M0 and M1 macrophages. C. Western blot showing the protein expression level of iNOS. D. METTL3 protein expression increased markedly in M1 macrophages compared to the M0 macrophage. E. The efficiency of METTL3 knockdown in RAW 264.7 cells confirmed by qRT-PCR and Western blot. F. qRT-PCR showing that METTL3 silencing decreased the mRNA level of IL-6 and iNOS in M1 macrophages. Data are analyzed with Student's t-test (two-tailed) and expressed as mean ± SEM. ***P < 0.001.

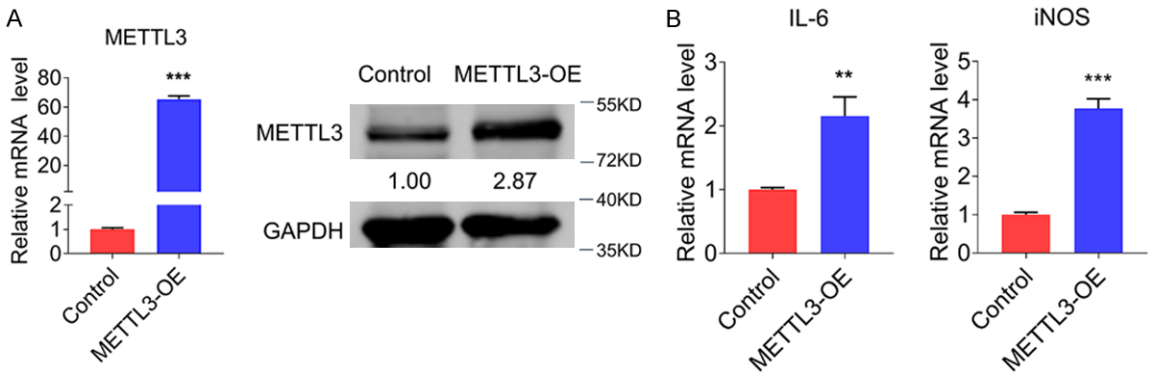

Figure 2. Overexpression of METTL3 promotes the polarization of M1 macrophage. (A) Verification of METTL3 overexpression at the mRNA level (left) and protein level (right) in RAW 264.7 cells. (B) qRT-PCR showing the mRNA expression level of IL-6 and iNOS increased by METTL3 forced expression in RAW 264.7 cells. Data are analyzed with Student's t-test (two-tailed) and expressed as mean ± SEM. **P < 0.005, ***P < 0.001.

rophage were characterized by the expression of IL-6 and iNOS in response to LPS stimulation for 24 h (**Figure 3B**). Consistent with what has mentioned previously, METTL3 expression was also increased in M1 macrophage polarized by BMDM (**Figure 3C**). To further demonstrate the METTL3-dependent effect on M1 macrophage polarization, we performed loss-of-function and gain-of-function assays. Knock-down or overexpression efficiency of METTL3 in BMDM were detected by qRT-PCR (**Figure 3D**, **3E**). M1 macrophage maker IL-6 mRNA expression was slight reduced with METTL3 knock-down (**Figure 3D**). Oppositely, METTL3 over-expression promoted IL-6 and iNOS mRNA expression, which mean the induction of M1 macrophage polarization (**Figure 3F**). In short, METTL3 plays the promotion role in differentiation of M1 macrophages both for RAW 264.7 and BMDM cells.

M1 macrophage differentiation facilitated by METTL3 arguments osteogenesis differentiation of bone marrow mesenchymal stem cells (BMSCs)

At the remodeling stage of bone fracture, macrophages secrete a repertoire of inflammatory and chemotactic mediators such as TNF-α, IL-1, IL-6, CCL2 to recruit BMSCs to the fracture site [18]. Additionally, M1 macrophages could enhance mineralization by BMSCs and bone healing through the pro-inflammation cytokines secretion involving OSM, TNF-α and IL-6 [7-9]. To further investigate the interaction between bone formation and macrophage polarization mediated by METTL3, we performed trans-well assays to evaluate the function of M1 phenotype macrophage on the migration of BMSCs. After transfected with METTL3 siRNA or METTL3 plasmid, we cultured RAW 264.7 cells (lower well) with BMSCs (upper well) in the trans-well systems with the M1 differentiation induced condition as descripted in **Figure 4A**. Our dates demonstrated that M1 macrophage with METTL3 knockdown inhibited BMSCs invasion ability compared with normal M1 macrophage. Oppositely M1 macrophage with METTL3 overexpression promoted BMSCs migration ability significantly (**Figure 4B**, **4C**). To further elucidate the in vivo significance of M1 polarization mediated by METTL3 in BMSCs osteogenic differentiation, we examined whether the osteogenic ability was changed when BMSCs cultured with the osteogenic induction medium which having RAW 264.7 cells supernatant culture medium. Alizarin red S (ARS) staining results illustrated that the supernatant culture medium of RAW 264.7 cells treated with LPS 24 h after METTL3 siRNA transfection observably inhibited the formation of osteogenic nodules compared to the siNC group (**Figure 4D**, **4E**). Conversely, osteogenic nodules were dramatically in METTL3 overexpression group. Collectively, M1 macrophage polarization accelerated by METTL3 plays a key role in controlling the osteogenic differentiation and migration of BMSCs *in vitro*.

M^{6}A-immunoprecipitation (RIP) microarray assays to identify potential targets of METTL3

Considering that BMDM is derived from BMSCs with the treatment of M-SCF, we used our previously published m^{6}A RNA immunoprecipitation

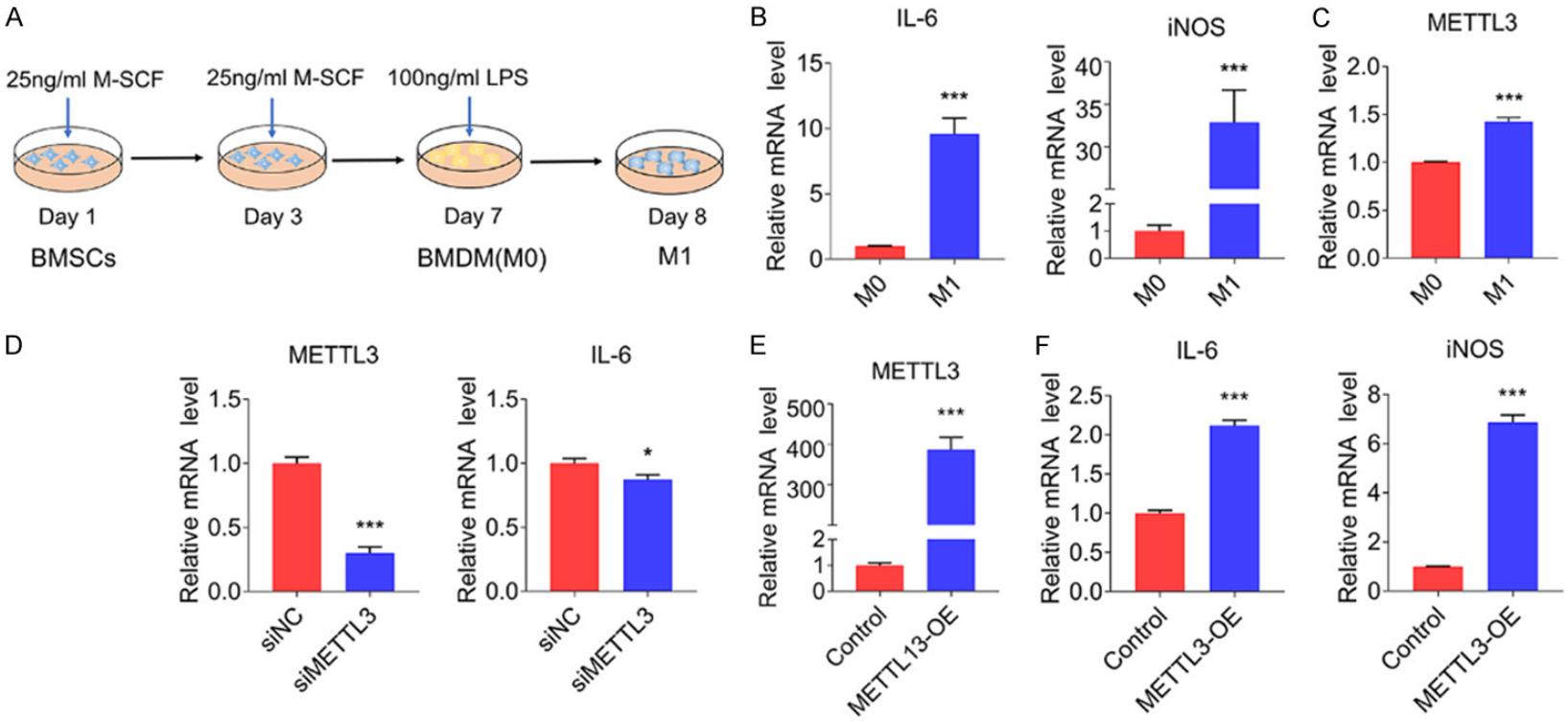

Figure 3. METTL3 promotes M1 macrophage polarization of BMDM. A. Schematic diagram presenting the procedure for the induction BMDM (M0 macrophage) from BMSCs and the polarization of M1 macrophages from BMDM. B. qRT-PCR results showing the mRNA expression level of IL-6 and iNOS in M0 and M1 macrophages. C. qRT-PCR results showing that METTL3 increased in M1 macrophage compared with M0 macrophage. D. qRT-PCR showing the verification of METTL3 knockdown in BMDM (left) and the expression level of IL-6 decreased by with METTL3 knockdown in M1 macrophage (right). E. The verification of METTL3 overexpression in BMDM detected by qRT-PCR. F. The mRNA expression level of IL-6 and iNOS increased with METTL3 overexpression. Data are analyzed with Student's t-test (two-tailed) and expressed as mean ± SEM. *P < 0.05, ***P < 0.001.

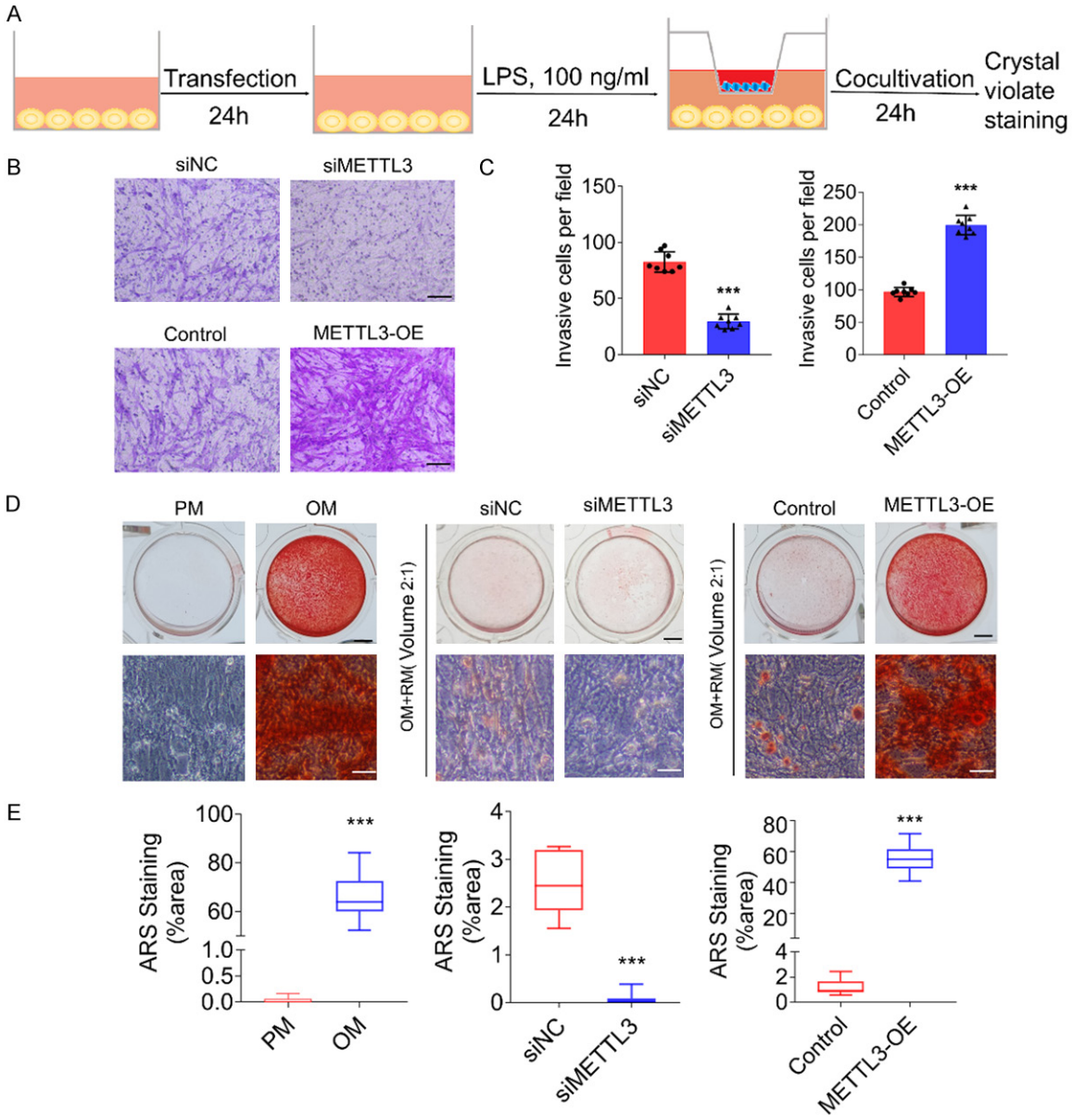

Figure 4. M1 macrophage stimulated by METTL3 promotes BMSCs migration and osteogenic differentiation ability. A. Schematic diagram showing the procedure of trans-well assays with RAW 264.7 cells and BMSCs co-cultured to evaluated the impact of M1 macrophage mediated by METTTL3 on BMSCs migration ability. B. Crystal violet staining representative image of trans-well assays. (bar: 100 μm). C. Bar graph representing the quantification of invasive cells (n=8). D. ARS staining shows effects of supernatant from different RAW 264.7 or not on osteogenic differentiation of BMSCs. PM: proliferation media; OM: osteogenic media (black bar: 2 mm; white bar: 50 μm). E. Typical examples of ARS staining showing the effects of M1 macrophage with METTL3 silencing or overexpression on BMSCs osteogenic differentiation ability. Data are analyzed with Student's t-test (two-tailed) and expressed as mean ± SEM. ***P < 0.001.

(RIP) microarray data [17] to identify the target mRNAs of METTL3 in siRNA negative control (siNC)- and siMETTL3-transfected BMSCs. Among 41,187 mRNAs detected, we identified 9,438 mRNAs m^{6}A modification decrease in METTL3 knockdown cells relative to those in the NC control cells (**Figure 5A**). Among these, there are 6 mRNAs which are the most strongly m^{6}A-mehylated (level > 0.4 in NC group) and they methylation was markedly decreased upon knockdown of METTL3 (> 3-fold decrease) (**Table 1**). Notably, dual-specificity phosphatase

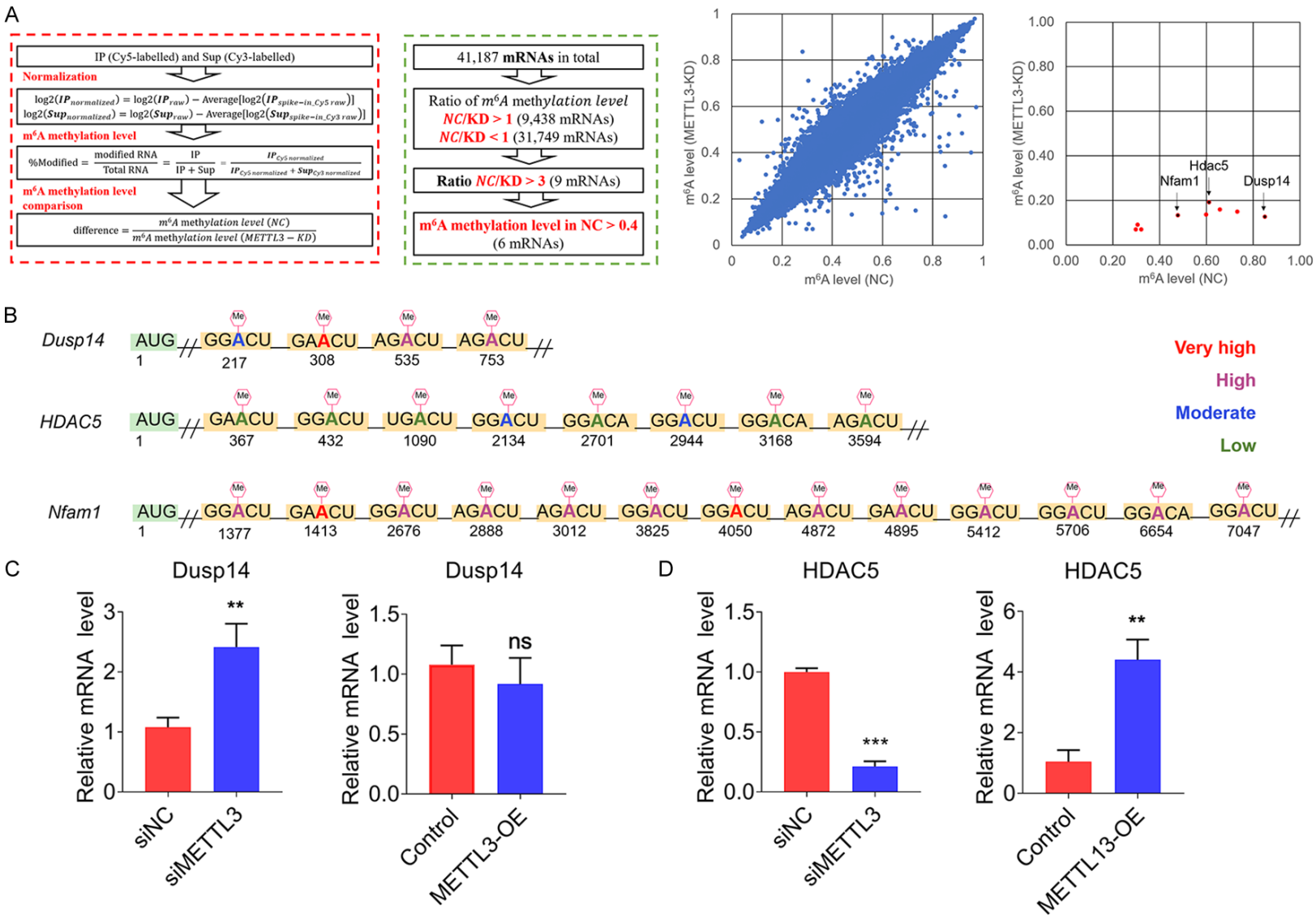

Figure 5. M^{6}A-immunoprecipitation (RIP) microarray identification of METTL3 targets. A. Schematic illustration of m^{6}A-RIP microarray analysis for RNA methylation flowchart showing the procedures for searching the METTL3 targets in BMSCs (left). Overview of totally different expression mRNA and the most obviously different expression mRNA in m^{6}A MeRIP-Seq (right). B. Potentially m^{6}A sites of Dusp14, HDAC5 and Nfam1 mRNA predicted by SRAMP program. C. The effects of METTL3 on the Dusp14 mRNA expression level in BMDM. D. The effects of METTL3 on the HDAC5 mRNA expression level in BMDM. Data are analyzed with Student's t-test (two-tailed) and expressed as mean ± SEM. **P < 0.005, ***P < 0.001.

Table 1. mRNA with METTL3-mediated m^{6}A methylation

Gene Symbol	siNC (IP)	siMETTL3 (IP)	siNC (Supernatant)	siMETTL3 (Supernatant)	siNC (Methylation Level)	siMETTL3 (Methylation Level)	Fold change (siMETTL3/siNC)
Dusp14	3.73	-1.30	1.22	1.50	0.85	0.13	6.78
Slc17a7	-2.69	-7.45	-4.14	-4.94	0.73	0.15	4.89
Kcnj14	3.64	-3.63	2.70	-1.24	0.66	0.16	4.12
Hdac5	4.44	-3.46	3.79	-1.38	0.61	0.19	3.20
Mpc1	3.75	-3.43	3.18	-0.77	0.60	0.14	4.38
Nfam1	-4.45	-4.90	-4.33	-2.18	0.48	0.13	3.61

14 (Dusp14), histone deacetylase 5 (HDAC5) and NFAT activating protein with ITAM motif 1 (Nfam1) are related to inflammation cytokine secretion and bone formation. To probe the mechanism by which m^{6}A methylation of Dusp14, HDAC5 and Nfam1 affects its processing *in vivo*, we sought to identify the position of the methylation site within the Dusp14, HDAC5 and Nfam1 mRNA [19-23]. Interestingly, they all carry potential m^{6}A modification sites according to a sequence-based SRAMP m6A modification site prediction web (http://www.cuilab.cn/sramp) (**Figure 5B** and Supplementary Figures 1, 2, 3). Therefore, we asked whether they are regulated by METTL3 during the processing of BMDM differentiation from BMSCs. Previous reports have revealed that Dusp14 alleviated inflammation by reduced the expression of IL-1β and TNF-α and protect bone loss via AMPKa-dependent manner [19, 20]. Dusp14 mRNA expression was significant down-regulated in BMDM and reversed by METTL3 silence, while there is no obvious change being detected with METTL3 overexpression (**Figure 5C**). Interestingly, the expression of HDAC5, a class IIa HDAC, was downregulated by METTL3 knockdown (**Figure 5D**). Previous studies have suggested a significant role of HDAC5 in osteogenic differentiation and osteoporosis progress [24, 25]. Li et al. have proofed that HDAC5 deficiency mice presented poor bone mineral density [26]. As expected, forced overexpression obviously reduced HDAC5 mRNA expression. Besides, the mRNA expression of Nfam1 is too low to be detected. Collectively, METTL3 mediated BMDM function in BMSCs osteogenesis and migration via targeting HDAC5.

Discussion

In the present study, we demonstrated that methyltransferase-like 3 (METTL3), a m^{6}A methyltransferase, participates M1 polarization of macrophages and further induces BMSCs migration and osteogenic differentiation, which are the critical beneficial factors for bone repair. We found that METTL3 expression was positively correlated with M1 polarization of macrophages. Moreover, M1 macrophage polarization promoted by METTL3 forced expression could obviously improve the migration and osteogenesis ability of BMSCs benefiting to the bone formation. In contrast, down-regulated of METTL3 produced the opposite effects. Moreover, METTL3 silence significantly reduced the m^{6}A modification of HDAC5, which has been reported to be a favorable factor for osteoporosis treatment [26]. Meanwhile, METTL3 depletion attenuated the expression of HDAC5 during the M1 polarization of macrophages. Collectively, our study demonstrates the functional importance of METTL3 in bone repair via targeting HDAC5 and modulating M1 macrophage polarization

Plenty of studies have demonstrated the strong association between m^{6}A modification and bone-related diseases such as osteoporosis, osteoarthritis and osteosarcoma. We have shown that METTL3 regulates BMSCs osteogenic differentiation via m^{6}A-based direct and indirect of RUNX2 [17]. In this previous work, we found that the expression of METTL3 were very low both in the bone tissues of osteoporosis patients and ovariectomized mice, increased dramatically during osteogenic differentiation in vitro. Therefore, it is possible that the increased expression of METTL3 may also contribute to the progression of bone repair.

Bone repair requires the involvement of multiple cells including osteoblast, osteoclast, monocyte such as preosteoclast and macrophage. Osteal macrophages (OsteoMacs) are a special subtype of macrophage residing in bone tissues which play vast and substantial

roles in bone biology due to their key function in bone formation and remodeling [27]. Current data indicates that polarization of macrophages toward either M1 or M2 subset phenotype could affect bone formation process directly or indirectly by their inflammation factor secretion [28]. Inflammatory cytokines secreted by macrophages could enhance BMSC mobilization to injured sites and osteogenic differentiation [29]. In the early steps of bone formation, the capabilities of BMSCs to display osteogenic differentiation and migrate to the fracture site play a crucial role [30]. Noticeably, METTL3 has reported to have important function in macrophage polarization, which could facilitate M1 macrophage polarization through the methylation of STAT1 mRNA [31, 32]. Nevertheless, it was still a puzzle whether m^6A methyltransferase METTL3 exerted effects on bone repair before the present study. In this study, we investigate that the expression of METTL3 increase with LPS treatment in macrophages. Besides, forced expression of METTL3 facilitates M1 macrophages polarization. Furthermore, we for the first time revealed that overexpression of METTL3 in M1 macrophages could accelerate the osteogenic differentiation of BMSCs when co-cultured with BMSCs. Consisting with our results, Yang et al. have proved that M1 macrophages secretes higher soluble factors oncostatin M (OSM) levels to promote the osteogenic differentiation of co-cultured BMSCs at the early time [33]. Meanwhile, inflammatory cytokines secreted by M1 macrophages, including TNF-α, IL-6, OSM, MCP-1, MIP-1α and IL-8 can accelerate the migration of BMSCs [34, 35]. Nevertheless, we have to point out that we do not discover the influence of METTL3 on M2 polarization in this study. To date there has been little agreement on the function of these two macrophage subtypes in osteogenic differentiation and migration ability of BMSCs. Recent studies have confirmed that M1 macrophages are the main immune cells at the first 3 days of bone injury, which will be gradually replaced by M2 macrophages. Additionally, Schlundt et al. discovered that the enhancement of M2 phenotype in macrophages at bone injury sites through IL-4 and IL-13 secretion promoted bone formation during the 3 weeks of investigation period [36]. Although not ignoring the function of M1 macrophages, these results suppose a more important function of M2 macrophages in bone repair [36]. Not with standing its limitation, this study does suggest METTL3 is beneficial to bone formation via modulating M1 macrophage differentiation. We will further explore the exact role of METTL3 in M2 macrophage differentiation in the future research.

Our m^6A-RIP-microarray demonstrated that the m^6A methylation modification levels of DUSP14, HDAC5 and Nfam1 were significantly decreased with METTL3 silencing, which have been reported to be related with bone formation or macrophage polarization modulation. Dusp14 is an atypical member of the DUSP proteins family, which has been verified to participate in a variety of pathogenesis, including oxidative stress and apoptosis and suppress various types of inflammatory cells [37-39]. Lei et al. have demonstrated that Dusp14 can prevent osteoclasts differentiation via elevating M-CSF/RANKL-elicited inflammation and apoptosis, which has an adverse impact on osteoporosis development. Although, in our study, we found that Dusp14 mRNA expression significant down-regulated in M1 macrophage polarization process which was reversed by METTL3 silence, there is no obvious change being detected with METTL3 overexpression. HDAC5, a class II HDACs, has been reported to participate the macrophage polarization [40] and has a promotion role in osteogenesis of BMSCs [22, 26]. Therefore, we hypothesized that M1 macrophage polarization promoted by METTL3 induce BMSCs osteogenesis and migration ability may by the means of expression changes of HDAC5. According to our results, knockdown of METTL3 reduced and overexpression of METTL3 enhanced the expression of HDAC in BMDM, which is positive collection with pro-inflammation cytokines (IL-6, iNOS). NFAM1 signaling is favorable for osteoclast formation and bone resorption activity in Paget's disease of bone [23]. However, the expression of Nfam1 was too low to be detected by qRT-RCR in M1 macrophage induced from BMDM with or without METTL3 siRNA or vector transfection. Thus, it is possible that the proliferation of M1 macrophages relies on the METTL3 signaling which is more responsive to LPS treatment, and the positive target of METTL3 is HDAC5.

In summary, our results suggest that METTL3 is a bone repair stimulating factor that could promote osteogenic differentiation and migra-

tion ability of BMSCs, working at least partially by enhancing the differentiation of M1 macrophage from M0 macrophage. We have also demonstrated that METTL3 silencing directly reduce the m^6A methylation of HDAC5 and down-regulated the mRNA expression of HDAC5, which has been reported to increase osteogenic genes expression and attenuate osteoporosis process [25]. Thus, METTL3 signaling might be considered a molecular target for the development of new strategies for the treatment of bone repair.

Acknowledgements

This work was supported by grants from the National Natural Science Fund of China (81972117), Heilongjiang Innovative Talent Training Fund for Young Teachers (UNPYSCT-2017073), Special Fund for the Development of Local Colleges and Universities supported by the Central Finance (Outstanding Young Talents Support Project, 0103/30011190007).

Disclosure of conflict of interest

None.

Address correspondence to: Lei Yang, Department of Orthopedics, The First Affiliated Hospital of Harbin Medical University, Harbin 150001, China. Tel: +86-13936183777; E-mail: yangray83@vip.qq.com; Dr. Ye Yuan, Department of Pharmacy, The Second Affiliated Hospital of Harbin Medical University, Harbin 150081, China. Tel: +86-13766864229; E-mail: yuanye_hmu@126.com

References

[1] Pajarinen J, Lin T, Gibon E, Kohno Y, Maruyama M, Nathan K, Lu L, Yao Z and Goodman SB. Mesenchymal stem cell-macrophage crosstalk and bone healing. Biomaterials 2019; 196: 80-89.

[2] Wang N, Gao J, Jia M, Ma X, Lei Z, Da F, Yan F, Zhang H, Zhou Y, Li M, He G, Meng J and Luo X. Exendin-4 induces bone marrow stromal cells migration through bone marrow-derived macrophages polarization via PKA-STAT3 signaling pathway. Cell Physiol Biochem 2017; 44: 1696-1714.

[3] Vi L, Baht GS, Whetstone H, Ng A, Wei Q, Poon R, Mylvaganam S, Grynpas M and Alman BA. Macrophages promote osteoblastic differentiation in-vivo: implications in fracture repair and bone homeostasis. J Bone Miner Res 2015; 30: 1090-1102.

[4] Zhou X, Li W, Wang S, Zhang P, Wang Q, Xiao J, Zhang C, Zheng X, Xu X, Xue S, Hui L, Ji H, Wei B and Wang H. YAP aggravates inflammatory bowel disease by regulating m1/m2 macrophage polarization and gut microbial homeostasis. Cell Rep 2019; 27: 1176-1189, e1175.

[5] Huang Y, Tian C, Li Q and Xu Q. TET1 knockdown inhibits porphyromonas gingivalis LPS/IFN-gamma-induced M1 macrophage polarization through the NF-kappaB pathway in THP-1 cells. Int J Mol Sci 2019; 20: 2023.

[6] Murray PJ. Macrophage polarization. Annu Rev Physiol 2017; 79: 541-566.

[7] Guihard P, Boutet MA, Brounais-Le Royer B, Gamblin AL, Amiaud J, Renaud A, Berreur M, Redini F, Heymann D, Layrolle P and Blanchard F. Oncostatin m, an inflammatory cytokine produced by macrophages, supports intramembranous bone healing in a mouse model of tibia injury. Am J Pathol 2015; 185: 765-775.

[8] Glass GE, Chan JK, Freidin A, Feldmann M, Horwood NJ and Nanchahal J. TNF-alpha promotes fracture repair by augmenting the recruitment and differentiation of muscle-derived stromal cells. Proc Natl Acad Sci U S A 2011; 108: 1585-1590.

[9] Xie Z, Tang S, Ye G, Wang P, Li J, Liu W, Li M, Wang S, Wu X, Cen S, Zheng G, Ma M, Wu Y and Shen H. Interleukin-6/interleukin-6 receptor complex promotes osteogenic differentiation of bone marrow-derived mesenchymal stem cells. Stem Cell Res Ther 2018; 9: 13.

[10] Wasnik S, Rundle CH, Baylink DJ, Yazdi MS, Carreon EE, Xu Y, Qin X, Lau KW and Tang X. 1,25-Dihydroxyvitamin D suppresses M1 macrophages and promotes M2 differentiation at bone injury sites. JCI Insight 2018; 3: e98773.

[11] Lu LY, Loi F, Nathan K, Lin TH, Pajarinen J, Gibon E, Nabeshima A, Cordova L, Jamsen E, Yao Z and Goodman SB. Pro-inflammatory M1 macrophages promote Osteogenesis by mesenchymal stem cells via the COX-2-prostaglandin E2 pathway. J Orthop Res 2017; 35: 2378-2385.

[12] Liu J, Yue Y, Han D, Wang X, Fu Y, Zhang L, Jia G, Yu M, Lu Z, Deng X, Dai Q, Chen W and He C. A METTL3-METTL14 complex mediates mammalian nuclear RNA N6-adenosine methylation. Nat Chem Biol 2014; 10: 93-95.

[13] Han J, Wang JZ, Yang X, Yu H, Zhou R, Lu HC, Yuan WB, Lu JC, Zhou ZJ, Lu Q, Wei JF and Yang H. METTL3 promote tumor proliferation of bladder cancer by accelerating pri-miR221/222 maturation in m6A-dependent manner. Mol Cancer 2019; 18: 110.

[14] Wang J, Ishfaq M, Xu L, Xia C, Chen C and Li J. METTL3/m(6)A/miRNA-873-5p attenuated oxidative stress and apoptosis in colistin-induced

kidney injury by modulating keap1/Nrf2 pathway. Front Pharmacol 2019; 10: 517.
[15] Lee H, Bao S, Qian Y, Geula S, Leslie J, Zhang C, Hanna JH and Ding L. Stage-specific requirement for Mettl3-dependent m(6)A mRNA methylation during haematopoietic stem cell differentiation. Nat Cell Biol 2019; 21: 700-709.
[16] Dorn LE, Lasman L, Chen J, Xu X, Hund TJ, Medvedovic M, Hanna JH, van Berlo JH and Accornero F. The N(6)-methyladenosine mRNA methylase METTL3 controls cardiac homeostasis and hypertrophy. Circulation 2019; 139: 533-545.
[17] Yan G, Yuan Y, He M, Gong R, Lei H, Zhou H, Wang W, Du W, Ma T, Liu S, Xu Z, Gao M, Yu M, Bian Y, Pang P, Li X, Yu S, Yang F, Cai B and Yang L. m(6)A methylation of precursor-miR-320/RUNX2 controls osteogenic potential of bone marrow-derived mesenchymal stem cells. Mol Ther Nucleic Acids 2019; 19: 421-436.
[18] Loi F, Cordova LA, Pajarinen J, Lin TH, Yao Z and Goodman SB. Inflammation, fracture and bone repair. Bone 2016; 86: 119-130.
[19] Hong L, Ai J and Ma D. Activation of Dusp14 protects against osteoclast generation and bone loss by regulating AMPKalpha-dependent manner. Biochem Biophys Res Commun 2019; 519: 445-452.
[20] Jianrong S, Yanjun Z, Chen Y and Jianwen X. DUSP14 rescues cerebral ischemia/reperfusion (IR) injury by reducing inflammation and apoptosis via the activation of Nrf-2. Biochem Biophys Res Commun 2019; 509: 713-721.
[21] Nishimori S, Lai F, Shiraishi M, Kobayashi T, Kozhemyakina E, Yao TP, Lassar AB and Kronenberg HM. PTHrP targets HDAC4 and HDAC5 to repress chondrocyte hypertrophy. JCI Insight 2019; 4: e97903.
[22] Li H, Xie H, Liu W, Hu R, Huang B, Tan YF, Xu K, Sheng ZF, Zhou HD, Wu XP and Luo XH. A novel microRNA targeting HDAC5 regulates osteoblast differentiation in mice and contributes to primary osteoporosis in humans. J Clin Invest 2009; 119: 3666-3677.
[23] Sambandam Y, Sundaram K, Saigusa T, Balasubramanian S and Reddy SV. NFAM1 signaling enhances osteoclast formation and bone resorption activity in Paget's disease of bone. Bone 2017; 101: 236-244.
[24] Baertschi S, Baur N, Lueders-Lefevre V, Voshol J and Keller H. Class I and IIa histone deacetylases have opposite effects on sclerostin gene regulation. J Biol Chem 2014; 289: 24995-25009.
[25] Xu D, Gao Y, Hu N, Wu L and Chen Q. miR-365 ameliorates dexamethasone-induced suppression of osteogenesis in MC3T3-E1 cells by targeting HDAC4. Int J Mol Sci 2017; 18: 977.
[26] Wein MN, Spatz J, Nishimori S, Doench J, Root D, Babij P, Nagano K, Baron R, Brooks D, Bouxsein M, Pajevic PD and Kronenberg HM. HDAC5 controls MEF2C-driven sclerostin expression in osteocytes. J Bone Miner Res 2015; 30: 400-411.
[27] Miron RJ and Bosshardt DD. OsteoMacs: key players around bone biomaterials. Biomaterials 2016; 82: 1-19.
[28] Horwood NJ. Macrophage polarization and bone formation: a review. Clin Rev Allergy Immunol 2016; 51: 79-86.
[29] Valles G, Bensiamar F, Maestro-Paramio L, Garcia-Rey E, Vilaboa N and Saldana L. Influence of inflammatory conditions provided by macrophages on osteogenic ability of mesenchymal stem cells. Stem Cell Res Ther 2020; 11: 57.
[30] Li C, Wang Q, Gu X, Kang Y, Zhang Y, Hu Y, Li T, Jin H, Deng G and Wang Q. Porous Se@SiO2 nanocomposite promotes migration and osteogenic differentiation of rat bone marrow mesenchymal stem cell to accelerate bone fracture healing in a rat model. Int J Nanomedicine 2019; 14: 3845-3860.
[31] Wang J, Yan S, Lu H, Wang S and Xu D. METTL3 attenuates LPS-induced inflammatory response in macrophages via NF-kappaB signaling pathway. Mediators Inflamm 2019; 2019: 3120391.
[32] Liu Y, Liu Z, Tang H, Shen Y, Gong Z, Xie N, Zhang X, Wang W, Kong W, Zhou Y and Fu Y. The N(6)-methyladenosine (m(6)A)-forming enzyme METTL3 facilitates M1 macrophage polarization through the methylation of STAT1 mRNA. Am J Physiol Cell Physiol 2019; 317: C762-C775.
[33] Zhang Y, Bose T, Unger RE, Jansen JA, Kirkpatrick CJ and van den Beucken J. Macrophage type modulates osteogenic differentiation of adipose tissue MSCs. Cell Tissue Res 2017; 369: 273-286.
[34] Anton K, Banerjee D and Glod J. Macrophage-associated mesenchymal stem cells assume an activated, migratory, pro-inflammatory phenotype with increased IL-6 and CXCL10 secretion. PLoS One 2012; 7: e35036.
[35] Fu X, Han B, Cai S, Lei Y, Sun T and Sheng Z. Migration of bone marrow-derived mesenchymal stem cells induced by tumor necrosis factor-alpha and its possible role in wound healing. Wound Repair Regen 2009; 17: 185-191.
[36] Schlundt C, El Khassawna T, Serra A, Dienelt A, Wendler S, Schell H, van Rooijen N, Radbruch A, Lucius R, Hartmann S, Duda GN and Schmidt-Bleek K. Macrophages in bone fracture healing: their essential role in endochondral ossification. Bone 2018; 106: 78-89.
[37] Hijikata M, Matsushita I, Le Hang NT, Thuong PH, Tam DB, Maeda S, Sakurada S, Cuong VC,

Lien LT and Keicho N. Influence of the polymorphism of the DUSP14 gene on the expression of immune-related genes and development of pulmonary tuberculosis. Genes Immun 2016; 17: 207-212.

[38] Xian F, Hu X, Hu XS, Chen QL, Qin J and Bie J. DUSP facilitates RPMI8226 myeloma cell aging and inhibited TLR4 expression. Eur Rev Med Pharmacol Sci 2018; 22: 6030-6034.

[39] Nakano Y. Novel function of DUSP14/MKP6 (dual specific phosphatase 14) as a nonspecific regulatory molecule for delayed-type hypersensitivity. Br J Dermatol 2007; 156: 848-860.

[40] Poralla L, Stroh T, Erben U, Sittig M, Liebig S, Siegmund B and Glauben R. Histone deacetylase 5 regulates the inflammatory response of macrophages. J Cell Mol Med 2015; 19: 2162-2171.

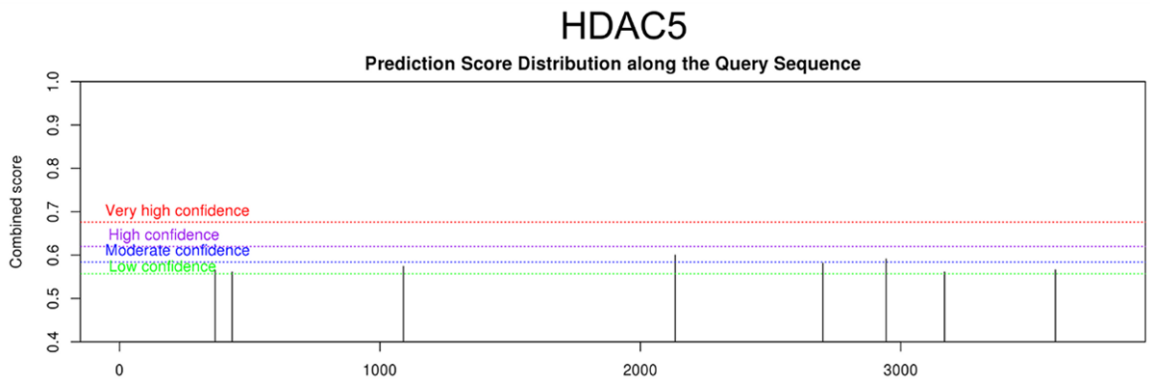

Supplementary Figure 1. The potential m^{6}A modification sites of HDAC5 mRNA predicted by SRAMP program.

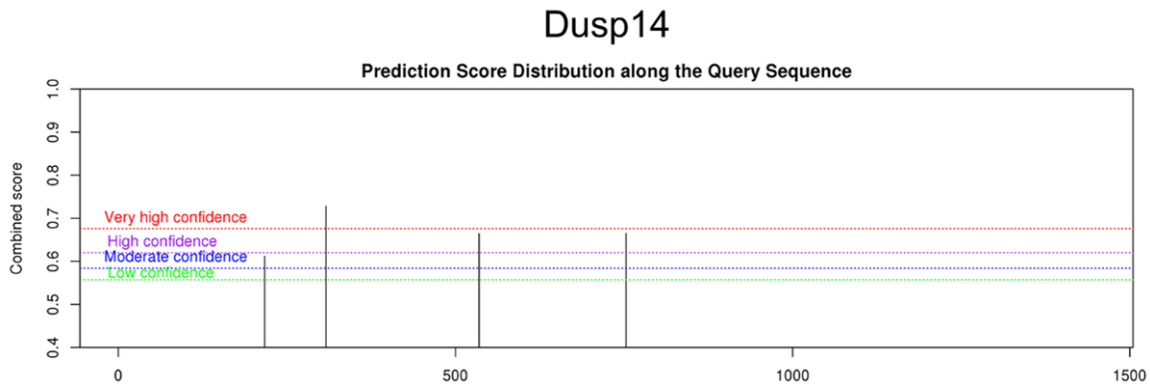

Supplementary Figure 2. The potential m^{6}A modification sites of Dusp14 mRNA predicted by SRAMP program.

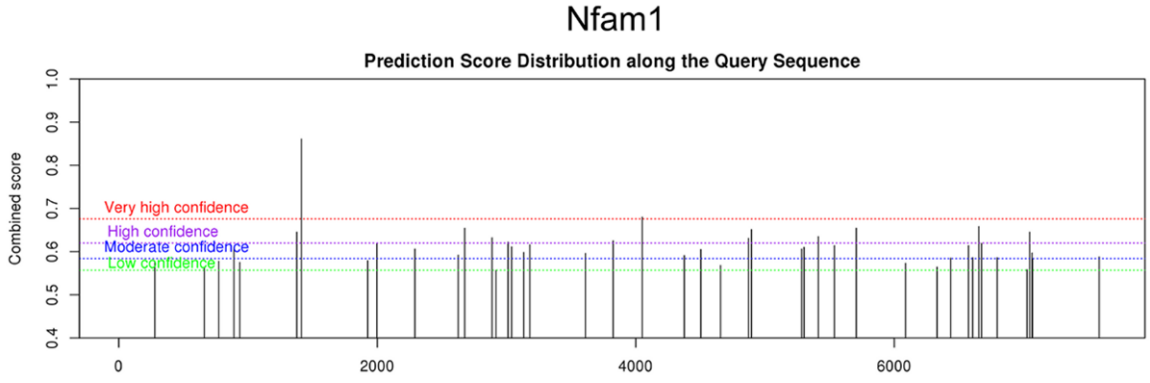

Supplementary Figure 3. The potential m^{6}A modification sites of Nfam1 mRNA predicted by SRAMP program.

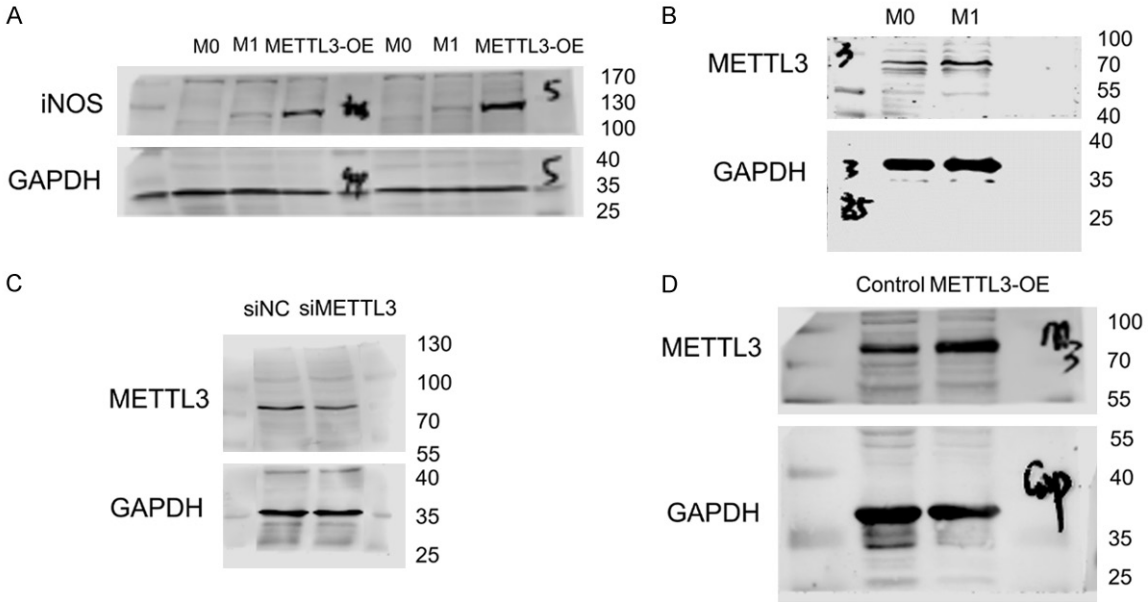

Supplementary Figure 4. The original, full-length gel images of **Figure 1C** (A), **Figure 1D** (B), **Figure 1E** (C) and **Figure 2A** (D).